Journal of Invertebrate Pathology 159 (2018) 49–60

Contents lists available at ScienceDirect

Journal of Invertebrate Pathology

journal homepage: www.elsevier.com/locate/jip

Morphology and molecular systematic of marine gregarines (Apicomplexa) from Southwestern Atlantic spionid polychaetes

S. Rueckert[a], N. Glasinovich[b], M.E. Diez[c], F. Cremonte[b], N. Vázquez[b,*]

[a] School of Applied Sciences, Edinburgh Napier University, Sighthill Campus, Sighthill Court, Edinburgh EH11 4BN, United Kingdom
[b] Laboratorio de Parasitología (LAPA), Instituto de Biología de Organismos Marinos (IBIOMAR-CONICET), Blvd. Brown 2915, Puerto Madryn, Argentina
[c] Laboratorio de Investigación en Informática (LINVI), Universidad Nacional de la Patagonia San Juan Bosco (UNPSJB), Blvd. Brown 3000, Puerto Madryn, Argentina

ARTICLE INFO

Keywords:
Gregarine parasites
Ultrastructure
Polyrhabdina
Selenidium
Phylogeny
Polychaetes
Argentina

ABSTRACT

Gregarines are a common group of parasites that infect the intestines of marine invertebrates, and particularly polychaetes. Here, we describe for the first time four gregarine species that inhabit the intestines of three spionid species: *Dipolydora* cf. *flava*, *Spio quadrisetosa* and *Boccardia proboscidea* from the Patagonian coast, Argentina, using light and scanning electron microscopy and molecular phylogenetic analyses of small subunit (SSU) rDNA sequences. Even though the spionid species thrive in the same environments, our results showed a high host specificity of the gregarine species. *Selenidium* cf. *axiferens* and *Polyrhabdina* aff. *polydorae* were both identified from the intestine of *D.* cf. *flava.* The new species, *Polyrhabdina madrynense* sp. n. and *Selenidium patagonica* sp. n., were described from the intestines of *S. quadrisetosa* and the invasive species *B. proboscidea,* respectively. All specimens of *D.* cf. *flava* and *S. quadrisetosa* were infected by gregarines (P = 100%), recording the highest mean intensity values of infection (MI = 80; 60 respectively), in contrast to *B. proboscidea* (P = 60%; MI = 38). We associated this finding with the recent invasion of this host. It is expected that in the future, an increase of its population density might favour a rising intensity of this gregarine infection.

1. Introduction

Gregarine apicomplexans are extracellular parasites that inhabit the intestines, coeloms and reproductive vesicles of marine, freshwater and terrestrial invertebrates (Rueckert et al., 2010). The systematics of this parasitic group is still under discussion, but they have traditionally been lumped into three major groups, the archigregarines, eugregarines and neogregarines based on their trophozoite (feeding stages) morphological features, host organisms and habitats (e.g. Grassé, 1953; Vivier and Desportes, 1990). Archigregarines occur exclusively in marine habitats, infect invertebrates and have trophozoites that resemble the general morphology of the infective sporozoite stages (e.g. Schrével, 1971; Kuvardina and Simdyanov, 2002; Leander et al., 2006; Schrével et al., 2016). Eugregarines occur in marine, freshwater and terrestrial habitats infecting a great diversity of invertebrates and have intestinal trophozoites that are significantly different in morphology and behaviour from sporozoites (e.g. Lord and Omoto, 2012). Neogregarines infect insects exclusively and they have reduced trophozoite stages. These parasites are associated with host tissues rather than the intestines per se (e.g. Sun et al., 2012). New species (i.e. morphotypes or phylotypes) of gregarines are generally discovered in previously unexplored host species, and closely related host species tend to be infected by closely related gregarine species (e.g. Levine, 1979; Rueckert and Leander, 2009; Simdyanov, 2009; Iritani et al., 2018).

Among marine invertebrates, polychaetes are a widespread and ecologically significant group in the benthic community (Fauchald, 1977; Rouse and Pleijel, 2001). Typically, they make up a large proportion of the intertidal invertebrate fauna (Cardell et al., 1999), where they play an important role in marine food chains. Many polychaetes are preyed upon by other polychaetes, a variety of marine invertebrates, as well as fishes and wading birds. In addition, they actively rework the sediment through ingestion and defecation (Nybakken and Bertness, 2005). In the coasts of north Patagonian gulfs, the species of the family Spionidae represent the largest and most common polychaetes in the benthic communities (Diez, com. pers.). Particularly, the alien polychaete species *Boccardia proboscidea,* which was introduced to the Southwestern Atlantic Ocean (Mar del Plata, Argentina) in 2008 (Jaubet et al., 2015), has recently been observed in a variety of substrates affecting the benthic community along the coasts of northern Patagonia (M.E. Diez unpublished data). Nevertheless, no studies on their parasite fauna on the Southwestern Atlantic coasts have been performed yet. In the present study, we describe for the first time

* Corresponding author.
E-mail address: nuria@cenpat-conicet.gob.ar (N. Vázquez).

https://doi.org/10.1016/j.jip.2018.10.010
Received 11 April 2018; Received in revised form 24 September 2018; Accepted 19 October 2018
Available online 24 October 2018

four gregarine species (Apicomplexa) from spionid polychaete hosts (*Dipolydora* cf. *flava*, *Spio quadrisetosa* and *B. proboscidea*) from the North Patagonian coast using light and scanning electron microscopy and molecular phylogenetic analyses of small subunit (SSU) rDNA sequences. In addition, prevalences and mean intensities of infection for each polychaete species are presented.

2. Material and methods

2.1. Collection and isolation of parasites

During autumn 2014, 600 specimens of spionid polychaetes (200 of each species: *Dipolydora* cf. *flava, Spio quadrisetosa* and *Boccardia proboscidea*) were collected in the intertidal zone of Puerto Madryn (42°20′S, 64°35′W), Chubut, Argentina. The polychaete species were identified under a stereomicroscope (Leica MZ 6). Each individual polychaete was placed on an object slide, covered with a cover slip and examined under the light microscope (Leica DM 2500) to count each trophozoite by scanning all the polychaete at 40× magnification. This was possible, as the polychaete hosts were translucent, which allowed for a clear identification of any gregarine trophozoites in the polychaete's intestine. Additionally, some trophozoites were isolated from the host's intestines, transferred into a Petri dish filled with seawater in order to wash off any residual host material, placed on an object slide covered with a cover slip and examined under the light microscope to be measured and photographed with the Leica DFC 280 digital camera. Some whole worm specimens as well as isolated gregarines were transferred into 4% formalin for scanning electron microscopy (SEM) preparation. Others were transferred to 1.5 ml microcentrifuge tubes filled with 95% ethanol and stored in a freezer for later DNA extraction.

2.2. Parasitological indices

Prevalence (P), intensity (I) and mean intensity (MI) of gregarines were calculated for each polychaete species according to Bush et al. (1997). Prevalence was calculated as the number of polychaetes infected, divided by the number of polychaetes examined. Intensity of infection was calculated as the number of gregarine trophozoites per polychaete and the mean intensity as the total number of trophozoites per polychaete divided by the number of infected polychaetes.

2.3. Light and scanning electron microscopy

Most of the light micrographs (LM) were produced using a Leica DM 2500 light microscope connected to a Leica DFC 280 digital camera. Some differential interference contrast (DIC) micrographs were taken with a 5 megapixel CMOS camera AxioCam Erc 5s, attached to an inverted microscope (Zeiss Axiovert 1).

For scanning electron microscopy (SEM), individual trophozoites of each polychaete species were dehydrated with a graded ethanol series (70%, 80%, 90%, 96% and 100% ethanol) for 15 min. The parasites were then submerged in hexamethyldisilazane (HMDS) for 5 min and left at room temperature for about 3 min. The HMDS was applied as an alternative method to the critical point drying using CO_2, in which liquids from the sample are removed by evaporation of HMDS at room temperature (Romero et al., 2011). The dried samples were sputter coated with gold/palladium using a sputter coater and observed with a scanning electron microscope (JEOL JSM-6460 LV). Other individuals were fixed for SEM following the classic SEM protocol including critical point drying as described for example in Rueckert and Leander (2010). Briefly, gregarines were fixed onto a 10 µm polycarbonate membrane filter (Millipore Corp., Billerica, MA) submerged in dH_2O. The cells were first exposed to OsO_4 vapors for 30 min, after which ten drops of 4% (w/v) OsO_4 were added directly to the dH_2O and the parasites were fixed for an additional 30 min. The filters were washed with water and dehydrated with a graded series of ethanol. They were critical point dried with CO_2. Filters were mounted on stubs, sputter coated with 5 nm of gold, and viewed under a scanning electron microscope (Hitachi S-4300). SEM data were presented on a black background using Adobe Photoshop CS5 (Adobe Systems Incorporated, San Jose, CA).

2.4. DNA isolation, PCR amplification and sequencing

Fixed trophozoites were washed three times with dH_2O and deposited into a 1.5 ml microcentrifuge tube. DNA was extracted using the MasterPureTM Complete DNA and RNA Purification Kit (Epicentre Biotechnologies, Madison, WI). Small subunit rDNA (SSU rDNA) sequences were PCR-amplified using a total volume of 25 µl containing 2 µl of primer, 2.5 µl of DNA template, 20.5 µl of dH_2O and one PuReTaq Ready-to-go PCR Bead (GE Healthcare, Quebec, Canada). The SSU rDNA sequences from these species were amplified in one fragment (~1800 base pairs) using universal eukaryotic PCR primers F1 (5′-GCGCTACCTGGTTGATCCTGCC-3′) and R1 (5′-GATCCTTCTGCAGGTTCACCTAC-3′). PCR was performed using the following protocol: After 4 cycles of initial denaturation at 94 °C for 4.30 min, 45 °C for 1 min and 72 °C for 1.45 min, 34 cycles of 94 °C for 30 sec (denaturation), 50 °C for 1 min (annealing), 72 °C for 1.45 min (extension), followed by a final extension period at 72 °C for 10 min. PCR products corresponding to the expected size were gel isolated using the UltraCleanTM 15 DNA Purification kit (MO Bio, Carlsbad, California) and cloned into the pSC-A-amp/kan vector using the StrataClone PCR Cloning Kit (Stratagene, Agilent Technologies, California). Eight cloned plasmids were digested with EcoRI and screened for size. Two clones were sequenced with ABI big dye reaction mix using vector primers and internal primers oriented in both directions using the cycle sequencing technology on an ABI 3730XL sequencing machine (Eurofins Genomics, Germany).

The new SSU rDNA sequences were initially identified by BLAST search and subsequently verified with molecular phylogenetic analyses (GenBank Accession numbers: *Polyrhabdina* aff. *polydorae* (MH697738), *Polyrhabdina madrynense* sp. n. (MH697739), *Selenidum* cf. *axiferens* (MH697737), *S. patagonica* sp. n. (MH697736).

2.5. Molecular phylogenetic analyses

The four new SSU rDNA sequences were aligned with 117 other SSU rDNA sequences, representing the major lineages of gregarines and dinozoans as relevant outgroup. The 121-sequence alignment was subsequently edited (ambiguously aligned regions and gaps were excluded manually) and fine-tuned using MacClade 4.08 (Maddison and Maddison, 2005). The program PhyML (Guindon and Gascuel, 2003) was used to analyse the 121-sequence alignment (1023 unambiguously aligned sites; gaps excluded) with maximum-likelihood (ML). Smart Model Selection (SMS) integrated into PhyML selected a general-time reversible (GTR) model of nucleotide substitutions (Posada & Crandall, 1998) that incorporated invariable sites and a discrete gamma distribution (four categories) (GTR + G + I model: $\alpha = 0.719$ and fraction of invariable sites = 0.194) under the Akaike Information Criterion (AIC) (Guindon et al., 2010). ML bootstrap analysis was performed on 100 pseudoreplicates, with one heuristic search per pseudo-replicate (Zwickl, 2006), using the same program set to the GTR model + G + I. Bayesian analysis of the 121-sequence dataset was performed using the program MrBayes 3.1.2 (Huelsenbeck and Ronquist, 2001). The program was set to operate using the following parameters: nst = 6, ngammacat = 5, rates = invgamma. Parameters of Metropolis Coupling Markov Chains Monte Carlo (mcmc) were set to: nchains = 4, nruns = 4, temp = 0.2, ngen = 7000000, samplefreq = 100, burninfrac = 0.5 (the first 50% of 70,000 sampled trees, i.e. the first 35000, were discarded in each run). The computation was performed on the CIPRES Science Gateway V 3.3 (Miller et al., 2010).

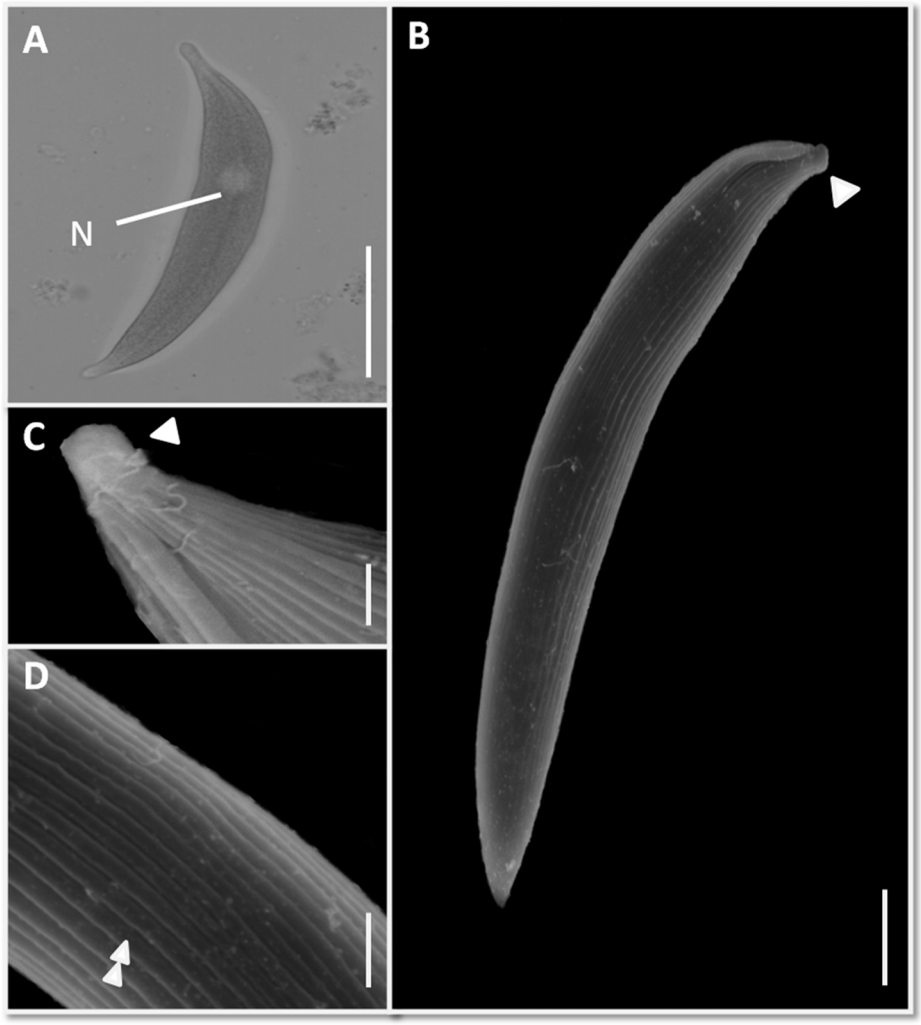

Fig. 1. General trophozoite morphology and surface ultrastructure of the gregarine *Selenidium* cf. *axiferens* in the spionid polychaete *Dipolydora* cf. *flava* showing: (A) trophozoite showing its nucleus (N) position (LM, DIC); (B) surface ultrastructure of the trophozoite with a knob-like mucron (arrowhead) (SEM); (C) higher magnification view of the mucron (arrowhead) (SEM); (D) higher magnification view of epicytical folds on the cell surface (double arrowhead) (SEM). Scale bars: A: 100 µm; B: 50 µm; C: 20 µm; D, E: 5 µm. The specimens in 1B-D were prepared following the hexamethyldisilazane protocol.

3. Results

Four gregarine species were found infecting *Dipolydora* cf. *flava* (Claparède, 1870), *Spio quadrisetosa* Blake, 1983 and *Boccardia proboscidea* Hartman, 1940 (Spionidae) as described below. All examined specimens of *D.* cf. *flava* and *S. quadrisetosa* were infected with gregarines, while it was only 60% of the *B. proboscidea* polychaetes. The highest mean intensity value of infection was recorded for *D.* cf. *flava* (MI 80 [16–100]), following *S. quadrisetosa* (MI 60 [12–100]), and finally *B. proboscidea* (MI 38 [2–100]).

3.1. Morphological descriptions by means of LM and SEM

All presented measurements were taken under the light microscope.

3.1.1. Host: Dipolydora cf. Flava

Selenidium* cf. *axiferens Fowell, 1936 (Fig. 1A–D). The trophozoites had a spindle-like shape (mean length = 211.39 µm [111.21–426.24 µm]; width = 33.11 µm [14.34–59.21 µm]; n = 15), with a broader middle section. The posterior end tapered into narrow rounded or flat-topped, knob-like tip, while the posterior end tapered into a pointed tip. The anterior end of the cell was slightly flattened up to the position of the nucleus. The flattened part of the trophozoite exhibited ridges on either side of the cell. The spherical nucleus (mean diameter = 17.86 µm [8.04–35.06 µm]; n = 15) was situated in the anterior part of the cell. A clearly visible axial channel ran from the mucron at the anterior end all the way to the posterior end, surrounding the nucleus. Scanning electron micrographs revealed 32–48 longitudinal epicytic folds with a density of ~1 fold/µm. The trophozoites showed bending and twisting motility.

Polyrhabdina* aff. *polydorae Léger, 1893 (Fig. 2A–E). Trophozoites presented an oval to ellipsoidal shape (mean length = 149.46 µm [89.53–297.20 µm]; width = 64.19 µm [33.78–135.28 µm]; n = 10), with rounded anterior and posterior ends. The spherical nucleus (mean = 22.16 µm [14.04–29.00 µm]; n = 10) was located in the central region of the cell. The mucron appeared either to be flat, or a rounded protrusion. The endoplasma had a brownish appearance, due to amylopectin storage products. The anterior end was free of granules, similar to the periphery of the trophozoite, revealing the ectoplasma. SEM micrographs demonstrated up to 190 longitudinal epicytic folds covering the surface of the cell with a density of 3–5 folds/µm at the widest point of the cell. The flat mucron in some of the cells appeared to be a fracture surface. The trophozoites were capable of gliding.

3.1.2. Host: Spio quadrisetosa

Polyrhabdina madrynense sp. n. (Fig. 3A–E). Trophozoites

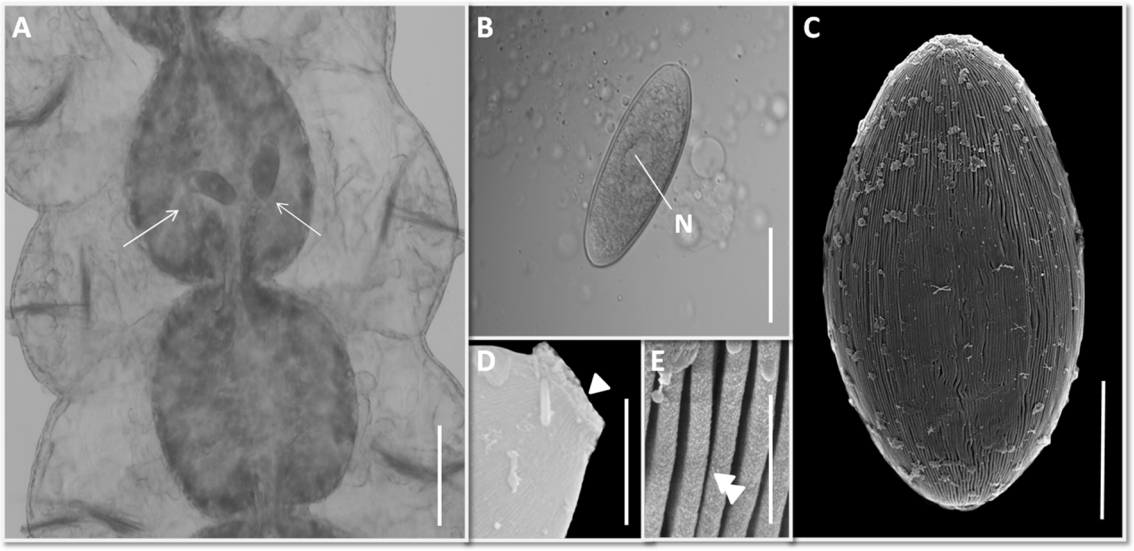

Fig. 2. General trophozoite morphology and surface ultrastructure of the gregarine *Polyrhabdina* aff. *polydorae* in the spionid polychaete *Dipolydora* cf. *flava* showing: (A) live trophozoites in intestine (arrows) (LM); (B) trophozoite showing its nucleus (N) position (LM, DIC); (C) general morphology of the trophozoite (SEM); (D) surface ultrastructure of the mucron area (arrowhead) (SEM); (E) higher magnification view of the epicytic folds on the cell surface (double arrowhead) (SEM). Scale bars: A: 100 µm; B, C: 50 µm; D: 10 µm; E: 1 µm. Specimens in 2C and 2D were prepared following the classic protocol with critical point drying. The specimen in 1E was prepared following the hexamethyldisilazane protocol.

presented rhomboid to ellipsoid shaped cells (mean length = 142.46 µm [30.61–384.53 µm]; width = 36.76 µm [9.73–75.71 µm]; n = 38), with rounded anterior and posterior ends. Some trophozoite stages showed knob-like protrusions, or flattened anterior ends. The spherical nucleus (mean = 13.33 µm [5.31–26.40 µm]; n = 38) was near one of the ends of the cell. The trophozoites were filled with brownish amylopectin storage products, except for the mucron area at the anterior end of the cell and the periphery of the cell. SEM micrographs revealed up to 150 longitudinal epicytic folds covering the entire surface of the cell with a density of 3–5 folds/µm except for the mucron area, which was free of folds. Some specimens possessed up to 10 prongs at the base of the mucron. The trophozoites showed gliding motility.

3.1.3. Host: Boccardia proboscidea

Selenidium patagonica sp. n. (Fig. 4A–F). Trophozoites presented a vermiform shape (mean length = 139.76 µm [111.63–170.14 µm]; width = 16.39 µm [10.48–20.06 µm]; n = 22), with a rounded anterior

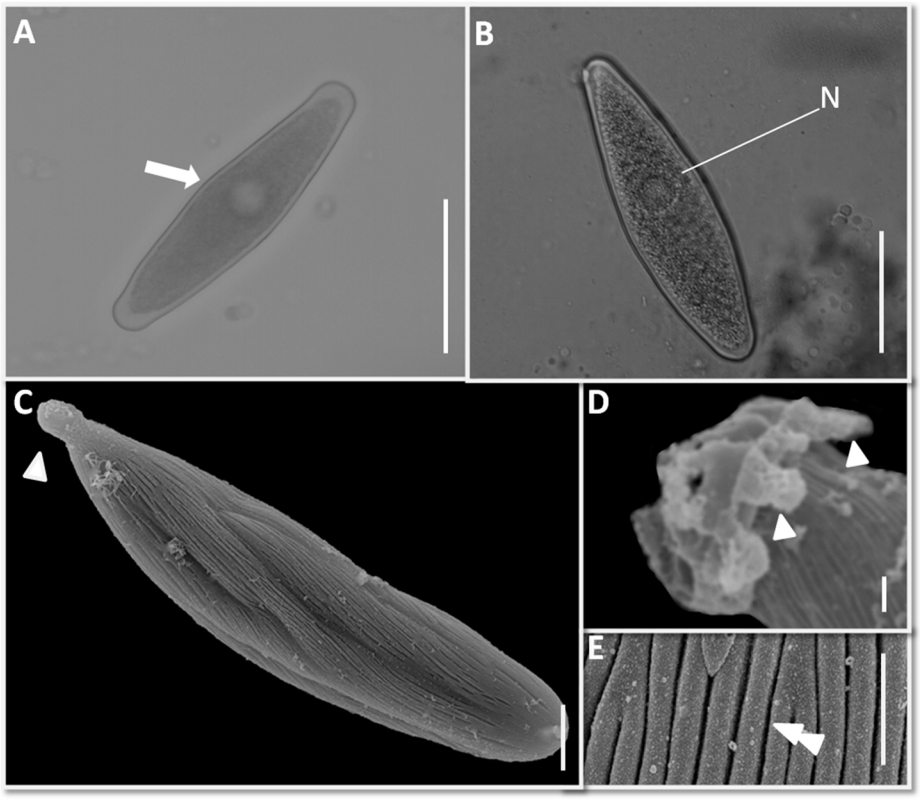

Fig. 3. General trophozoite morphology and surface ultrastructure of the gregarine *Polyrhabdina madrynense* sp. n. in the spionid polychaete *Spio quadrisetosa* showing: (A) ellipsoid shaped trophozoite (arrow) (LM); (B) trophozoite showing its spherical nucleus (N) position (LM, DIC); (C) surface ultrastructure of the trophozoite with and without a rounded protrusion mucron (arrowhead) (SEM); D) higher magnification view of a mucron with prongs (arrowhead); (E) higher magnification view of the epicytic folds on the cell surface (double arrowhead) (SEM). Scale bars: A, B: 50 µm; C: 10 µm; D, E: 1 µm. The specimen in 3E was prepared following the classic protocol with critical point drying. Specimens in 3C-D were prepared following the hexamethyldisilazane protocol.

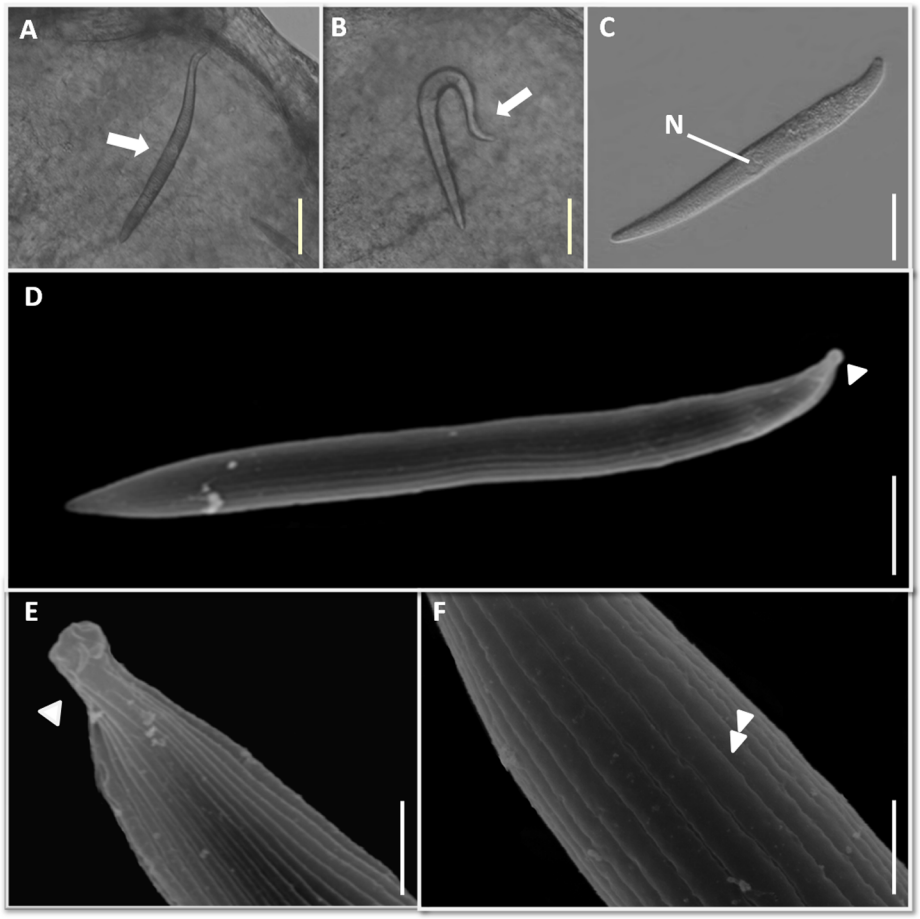

Fig. 4. General trophozoite morphology and surface ultrastructure of the gregarine *Selenidium patagonica* sp. n. in the spionid polychaete *Boccardia proboscidea* showing: (A) live trophozoite (arrow) in intestine (LM); (B) trophozoite showing flexion and torsion type mobility (arrow); (C) trophozoite showing its nucleus (N) position (LM, DIC); (D) surface ultrastructure of the trophozoite showing a pointed mucron (arrowhead) (SEM); (E) higher magnification view of the mucron (arrowhead) (SEM); (F) higher magnification view of epicytical folds on the cell surface (double arrowhead) (SEM). Scale bars: A, B: 50 µm; C: 30 µm; D: 20 µm, E, F: 5 µm. Specimens in 4D-F were prepared following the hexamethyldisilazane protocol.

end sometimes showing a slight protrusion and a tapered posterior end. *In situ* the anterior halves of the cells looked more slender. The spherical nucleus (mean = 11.15 µm [7.98–16.21 µm]; n = 22) was located in the central region of the cell. SEM micrographs demonstrated 22–28 longitudinal epicytic folds covering the surface of the cell with a density of ~1 folds/µm. The mucron was quite slender, protruding with a rounded to flat knob-like top, free of folds. The trophozoites were capable of bending and twisting.

3.2. Molecular phylogeny of gregarine apicomplexans in spionid polychaetes

We were able to obtain four SSU rDNA sequences, two for species of the genus *Selenidium* and for the first time two of the genus *Polyrhabdina*. Molecular phylogenetic analyses of the 121-sequence dataset produced a tree with a moderately supported outgroup consisting of dinoflagellates and one environmental sequence, and a moderately supported clade of apicomplexans (Fig. 5). The backbone of the tree was very poorly resolved. The ingroup of apicomplexans formed four distinct clades (three large, one small) consisting of (1) cryptosporidians and eugregarines of the genus *Polyrhabdina* from polychaete hosts, (2) piroplasmids and coccidians, (3) monocystids, neogregarines, rhytidocystids and eugregarines from terrestrial hosts, (4) archi- and eugregarines from marine hosts. The new sequences of *Selenidium patagonica* sp. n. from *Boccardia proboscidea* and *Selenidium* cf. *axiferens* from *Dipolydora* cf. *flava* clustered together in a weakly supported clade containing the type species *Selenidium pendula*. The two *Polyrhabdina* SSU rDNA sequences (one sequence from *Polyrhabdina* aff. *polydorae* from *Dipolydora* cf. *flava* and one from *Polyrhabdina madrynense* sp. n. from *Spio quadrisetosa*) formed a clade with three *Cryptosporidium* sequences, but with no support. This clade clustered as sister group to all other apicomplexans with moderate support.

A pairwise distance calculation based on the Kimura two-parameter model (Kimura, of 1560 nt (with complete deletion of gaps) resulted in sequence divergences between 1% and 15% between all *Selenidium* species within the clade of the type species *S. pendula* (Table 1). The sequence divergence between the new sequence of *S.* cf. *axiferens* and the other *Selenidium* species ranged between 5% and 13%, while the sequence divergence for the sequence of the new species *S. patagonica* sp. n. ranged between 1% and 12% when compared to the other *Selenidium* species in this clade.

4. Discussion

To date parasitological studies on polychaete species in South America were not available. This study describes two novel species of gregarines: *Polyrhabdina madrynense* sp. n. in *Spio quadrisetosa* and *Selenidium patagonica* sp. n. in the invasive species *Boccardia proboscidea*. Two of the isolated gregarines belong to the genus *Selenidium* and two to the genus *Polyrhabdina*. The genus *Selenidium* belongs to the archigregarines, a group of poorly understood marine gregarines that are inferred to be the most ancestral of all gregarine species. This group is important for the understanding of the gregarine evolution, but probably also the evolutionary history of the apicomplexans as a whole (Leander, 2007, 2008; Wakeman and Leander, 2012; Rueckert and Horàk, 2017). The trophozoites of archigregarines possess only a few epictic folds, ranging from 4 to about 50 and undergo active bending and coiling movements. The *Selenidium* species isolated from the intestine of *D.* cf. *flava* agreed in host species and general morphology with the original and subsquent descriptions of *S. axiferens* Fowell, 1936 (Table 2). One of the prominent morphological features is the axial channel/'axial duct'/'Fowell's duct' that runs from the anterior to the posterior end surrounding the nucleus (Fowell, 1936a, b; Desportes

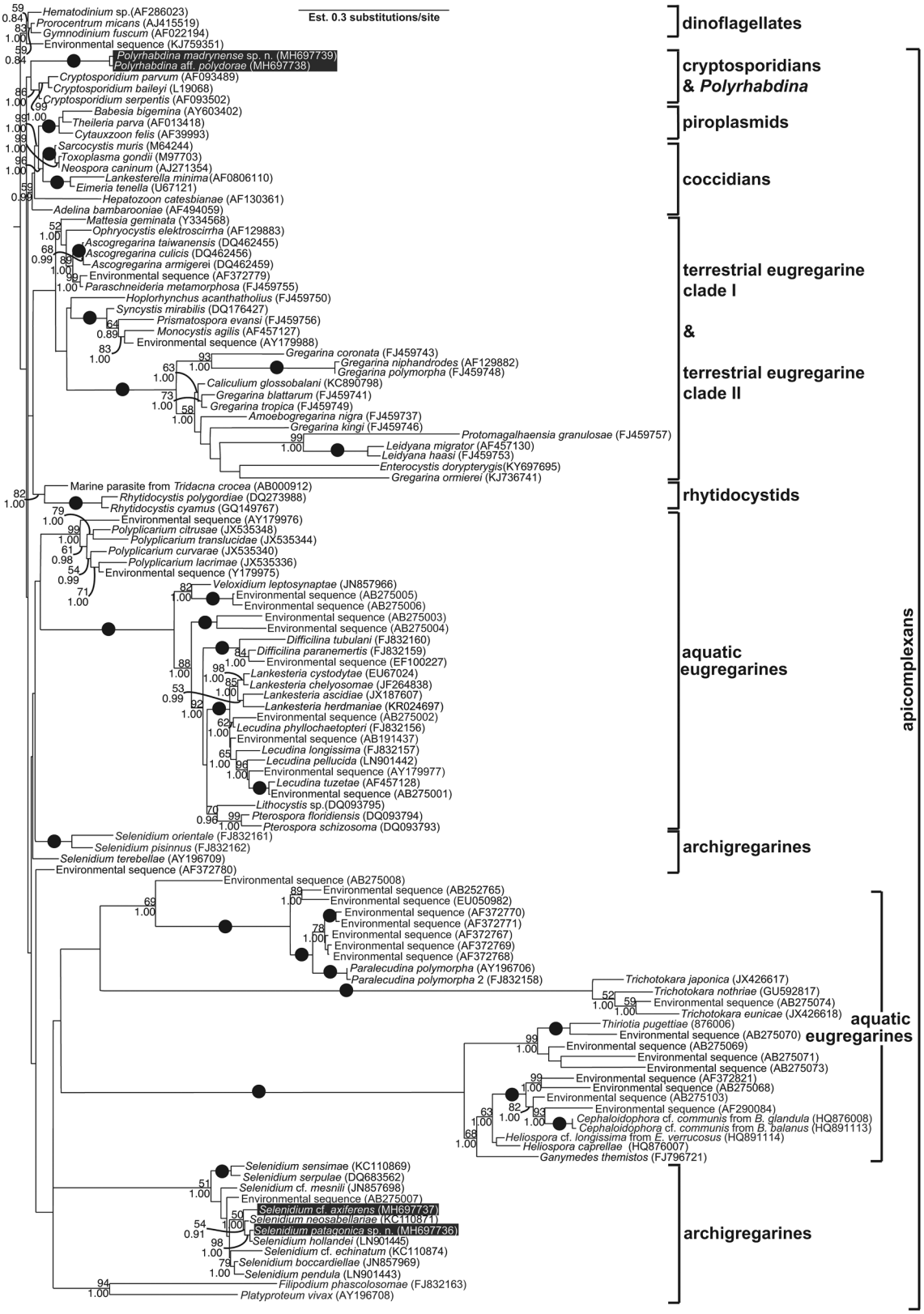

Fig. 5. Phylogenetic tree of gregarine apicomplexans. The tree includes core apicomplexans and dinoflagellate species were used as outgroup. This gamma-corrected maximum likelihood tree (AIC = 0.55708.27652, α = 0.719, fraction of invariable sites = 0.194, 4 rate categories) was inferred using the GTR + G + I model of substitution on an alignment of 121 small subunit (SSU) rDNA sequences and 1028 unambiguously aligned sites. Numbers at the branches denote bootstrap percentage (top) and Bayesian posterior probabilities (bottom). When either value was below 50% or 0.50, numbers were not reported. Black dots on branches denote Bayesian posterior probabilities and bootstrap percentages of 1.00/100% or higher.

Table 1
Estimates of evolutionary divergence between SSU rDNA sequences from *Selenidium* species including new sequences (highlighted in bold) from Patagonia, Argentina.

	Selenidium sensimae	*Selenidium* cf. *echinatum*	*Selenidium neosabellariae*	*Selenidium* cf. *mesnili*	***Selenidium* cf. *axiferens***	***Selenidium patagonica* sp. n.**	*Selenidium boccardiellae*	*Selenidium serpulae*	*Selenidium pendula*	*Selenidium hollandei*
Selenidium sensimae										
Selenidium cf. *echinatum*	0.14									
Selenidium neosabellariae	0.12	0.12								
Selenidium cf. *mesnili*	0.11	0.12	0.09							
Selenidium* cf. *axiferens	0.13	0.13	0.05	0.10						
***Selenidium patagonica* sp. n.**	0.12	0.12	0.03	0.09	0.05					
Selenidium boccardiellae	0.11	0.10	0.08	0.08	0.10	0.08				
Selenidium serpulae	0.06	0.13	0.10	0.09	0.12	0.11	0.10			
Selenidium pendula	0.12	0.10	0.09	0.09	0.10	0.09	0.04	0.11		
Selenidium hollandei	0.13	0.12	0.03	0.09	0.05	0.01	0.09	0.11	0.09	

Grey color shows the sequence divergence between the new sequence of *S. axiferens* and the other *Selenidium* species and the sequence divergence for the sequence of the new species *S. boccardiae* sp. n. compared to the other *Selenidium* species in this clade.

and Schrével, 2013; Schrével and Desportes, 2013). This axial channel has also been reported from *S. pendula* and *S. spionis* (Fowell, 1936a, b). Some of the isolated specimens were a bit larger than the described range for *S. axiferens*, but the number of the trophozoite's epicytic folds described here was similar again. Most of the other *Selenidium* species are less wide and have fewer longitudinal epicytic folds (see Table 2). This evidence strongly suggests that our isolated specimens are *S. axiferens* species. As our host specimens did not originate from the type locality (East Atlantic), we have decided to designate our gregarine isolate the name *S.* cf. *axiferens*, until sequence data become available from *S. axiferens* isolated from *D. flava* at the type locality. The novel species *S. patagonica* sp. n. described from *B. proboscidea* has vermiform trophozoites that fall in the size-range of most other *Selenidium* species (Table 2). The number of epicytic folds was most similar to *S. pendula*, *S.* cf. *mesnili* and *S. spionis*. Apart from the fact that they are infecting different host species, the trophozoites described were smaller than those of *S. pendula*; compared to *S.* cf. *mesnili* the nucleus was spherical and situated in the middle and not ellipsoidal and shifted away from the middle, while *S. spionis* has a rounded or spoon-like mucron and not a pointed one (Table 2). The sequence divergence calculations showed a divergence of 9% between SSU rDNA sequences from *S. patagonica* sp. n. and both *S. pendula* and *S.* cf. *mesnili*. Based on the differences in described characteristics we established the new species for the isolated trophozoites from *B. proboscidea*.

The trophozoites of intestinal eugregarines (e.g. lecudinids and septate gregarines) can possess hundreds of epicytic folds that significantly increase the surface area. Due to the numerous folds, the eugregarine cells become stiff and they usually show gliding rather than bending or twisting movements. Morphological descriptions of eugregarines of the genus *Polyrhabdina* based on scanning electron microscopy were not available yet. We identified *Polyrhabdina* aff. *polydorae* from the intestine of *Dipolydora* cf. *flava*. As the morphological characteristics were most closely to the previously described *P. polydorae* from two host species *Polydora ciliata* and *D. flava* (Léger, 1893; Mackinnon and Ray, 1931), but not identical due to the missing prongs and the larger size, we decided to use *P.* aff. *polydorae* (Table 3). It is unlikely that *D.* cf. *flava* would be host to another very similar gregarine species. Most of the species descriptions within the genus *Polyrhabdina* are quite scanty (Table 3, Caullery and Mesnil, 1914; Ganapati, 1946), making a comparison of newly isolated with already described species difficult. Most of the descriptions are relying on line drawings only, if figures are at all presented (Caullery and Mesnil, 1914). Until the sequence data of these previously described *Polyrhabdina* species become available, it is sensible to use *P.* aff. *polydorae*. Here, we are able to present for the first time SEM and SSU rDNA sequence data, expanding our knowledge of surface ultrastructure and phylogenetic relationships of this species. While gregarines belonging to the genus *Polyrhabdina* have been described already from spionid polychaetes, none have been described so far for *Spio quadrisetosa*. The isolated gregarine species confirmed to the overall characteristics of the genus *Polyrhabdina*, but there were some obvious differences. The shape of the trophozoites was ellipsoid to rhomboid compared to the mostly pear- or sack-like appearance (Table 3, Mackinnon and Ray, 1931). Cells could reach up to almost 400 × 75 µm, the largest size that has been reported so far. The size of the spherical nucleus and its position towards the ends of the cell are also setting this new species apart. The SEM revealed 80–150 longitudinal epicytic folds that have not been reported before for any species, as SEM data are not available for the genus *Polyrhabdina*. There are around 10 prongs visible at the anterior end of some trophozoites, which is comparable to *P. spionis*, *P. brasili* and *P. minuta*, but this remains the only similar morphological characteristic. Therefore, we have established the new species *P. madrynense* sp. n. We were also able to obtain the SSU rDNA sequence for this species.

While there are around 40 SSU rDNA reference sequences available for *Selenidium* species in public databases like GenBank, there is none available to date for any species within the genus *Polyrhabdina*. In general, the support values for Bayesian posterior probability were stronger than the ML bootstrap values (Fig. 5). Our phylogenetic analyses placed *S.* cf. *axiferens* and *S. patagonica* sp. n. in the *Selenidium* clade around the type species *S. pendula*. This clade encompasses 10 species in total that infect spionid (3) as well as sabellid (4), sabellariid (2) and cirratulid (1) polychaetes and one environmental sequence. In this clade our new sequences formed a clade with *S. neosabellariae* and *S. hollandei*. *Selenidium patagonica* sp. n. clustered together with *S.*

Table 2
Morphological comparison of *Selenidium* (Apicomplexa) species presented in this study (highlighted in bold) and other species that belong to the same clade in the phylogenetic tree or are from spionid hosts.

Selenidium species	Polychaete host (accepted names)	Locality	Trophozoite shape	Trophozoite size (LxW. μm)	Nucleus shape	Nucleus size (L × W. μm)	Position of nucleus	Motility	N of long. epicytic folds	Transverse surface folds	Shape of mucron	SSU rDNA sequence available	Literature
S. pendula Giard, 1884	*Scolelepis squamata* (Müller, 1806)	E. Atlantic	Spindle-shaped	150–400 × 30–40	Round to oval	18–33 × 13–32	Middle	Bending, twisting, pendulum-like	20–30	Unknown	Pointed	Yes	Giard (1884), Schrével (1970), Levine (1971), Schrével et al. (2016)
S. hollandei Vivier & Schrével, 1966	*Sabellaria alveolata* Linnaeus, 1767	E. Atlantic	Spindle-shaped, elongate, flattened	up to 500 × 20–30	Spherical or ovoid	16 × 6–8	Unknown	Bending, twisting	About 16	Unknown	Heart-shaped	Yes	Vivier and Schrével (1966), Schrével (1970)
S. serpulae Lankester, 1863	*Serpula vermicularis* Linnaeus, 1767	W. Pacific	Spindle-shaped	100–150 × 7–25	Ellipsoidal	7–10 × 5–11	Anterior half	Bending, twisting, contract/ stretch	14–23	Yes	poInted to round	Yes	Levine (1971), Leander (2006)
S. neosabellariae Wakeman & Leander, 2013	*Neosabellaria cementarium* (Moore, 1906)	W. Pacific	Vermiform	125–350 × 9–12	Spherical	10	Middle	Bending, twisting, undulated	10–12	Yes	Nipple-shaped	Yes	Wakeman and Leander (2013)
S. cf. *mesnili* Brasil, 1909	*Myxicola infundibulum* (Montagu, 1808)	W. Pacific	Spindle-shaped	85–157 × 18–24	Ellipsoidal	7–9 × 10–11	Anterior to posterior	Bending, coiling	22–24	Yes	Pointed to round	Yes	Brasil (1909), Wakeman and Leander (2012)
S. boccardiellae Wakeman & Leander, 2012	*Boccardiella ligerica* (Ferronnière, 1898)	W. Pacific	Spindle-shaped, partially flattened	87–250 × 10–12	Ellipsoidal	10–12 × 4–6	Anterior half	Bending, Coiling, thrashing	10–12	No	Pointed	Yes	Wakeman and Leander (2012)
***S. patagonica* sp. n.**	***Boccardia proboscidea*** Hartman, 1940	**SW. Atlantic**	**Vermiform**	**112–170 × 11–20**	**Spherical**	**8–16**	**Middle**	**Bending, twisting**	**22–28**	**No**	**Pointed**	**Yes**	**This study**
S. sensimae Wakeman & Leander, 2013	*Spirobranchus giganteus* (Pallas, 1766)	E. Pacific	Spindle-shaped	130–170 × 10–13	Ellipsoidal	10 × 4–6	Middle	Slow bending, twisting	16–18	no	Rounded to blunt	Yes	Wakeman and Leander (2013)
S. cf. *echinatum* Caullery & Mesnil, 1899	*Dodecaceria concharum* Örsted, 1843	W. Pacific	Spindle-shaped	95–205 × 8–11	Spherical	10	Anterior half	Bending, twisting	10–12	no	Nipple-shaped	Yes	Caullery and Mesnil (1899); Wakeman and Leander (2013)
S. axiferens Fowell, 1936	*Dipolydora flava* Claparède, 1870	E. Atlantic	Spindle-shaped	155–300 × 14–31	Ellipsoidal		Anterior half	Bending, folding	30–45	Unknown	Knob-like	No	Fowell (1936a, b)
S. cf. *axiferens* Fowell, 1936	***Dipolydora* cf. *flava*** Claparède, 1870	**SW. Atlantic**	**Spindle-shaped, partially flattened**	**111–462 × 14–59**	**Spherical**		**Anterior half**	**Bending, wisting**	**32–48**	**No**	**Knob-like**	**Yes**	**This study**
S. spinosis Ganapati, 1946	*Prionospio cirrifera* Wirén,1883	N. Indian Ocean	Spindle-shaped	60–80 × 10–12	Spherical		Anterior half	Bending, folding	10	Unknown	Rounded with sucker-like depression	No	Ganapati (1946), Levine (1971)
S. spionis (von Kölliker, 1845)	*Malacoceros fuliginosus* (Claparède, 1870) *Spio martinensis* Mesnil, 1896	E. Atlantic	Spindle-shaped	30–300 × 25–50	Oval		Middle	Bending, folding	20–30	Unknown	Rounded or spoon-shaped	No	Ray (1930), Schrével (1971), Levine (1971)
S. foliatum Ray, 1930	*Malacoceros fuliginosus* (Claparède, 1870)	White Sea	Flattened, leaf-like	30–250 × 10–25	Ovoid	8 × 5	Middle	Snake- or pendulum-like	16–24	Unknown	Rounded with cone-like depression	No	Ray (1930), Schrével (1971)

(*continued on next page*)

Table 2 (*continued*)

Selenidium species	Polychaete host (accepted names)	Locality	Trophozoite shape	Trophozoite size (LxW. µm)	Nucleus shape	Nucleus size (L × W. µm)	Position of nucleus	Motility	N of long. epicytic folds	Transverse surface folds	Shape of mucron	SSU rDNA sequence available	Literature
S. polydorae Ganapati, 1946	*Polydora ciliata* (Johnston, 1838)	N. Indian Ocean	Spindle-shaped	100–150 × 8–12	Ellipsoidal/ ovoidal	Unknown	Anterior half	Wriggling, twisting.	10–22	Unknown	Nipple-like	No	Ganapati (1946), Levine (1971)

hollandei with strong support. These species are morphologically quite different, as *S. hollandei* is extremely elongated and flattened, with heart-shaped anterior end (Schrével, 1970; Schrével et al., 2016; Rueckert and Horàk, 2017), and it infects a sabellariid polychaete, whereas *S. boccardiae* sp. n. is infecting a spionid polychaete. *Selenidium* cf. *axiferens*, also from a spionid polychaete, clustered as sister to the other three species. The host of *S. neosabellariae* was a sabellariid polychaete. Overall, our new sequences from gregarines infecting spionid polychaetes did not cluster with the other available sequences of spionid infecting gregarines such as *S. pendula* and *S. boccardiellae*. Therefore, the clustering of the *Selenidium* sequences in the *Selenidium* type species clade does not directly reflect host affinity, which had been suggested in previous studies (e.g. Wakeman and Leander, 2013; Schrével et al., 2016). Even though more sequences are available to date, there is still the need to enlarge the sample size of the genus *Selenidium,* and to employ additional molecular markers (e.g. LSU rDNA, COI, HSP90), which has also been suggested previously (Wakeman and Leander, 2013; Rueckert and Horàk, 2017) to better resolve the deeper branches of these phylogenetic trees for an improved understanding of the relationships within the archigregarines and their role in the evolutionary history of the gregarines and probably the Apicomplexa as a whole.

The phylogenetic position of the two new *Polyrhabdina* sequences is interesting as they form a clade with three *Cryptosporidium* species, but this clade is not supported and therefore very speculative. The clustering of *P.* aff. *polydorae* and *P. madrynense* sp. n. is highly supported. The genus *Polyrhabdina* belongs to the family Lecudinidae in the Eugregarinorida. All of the characteristics of the genus *Polyrhabdina* are eugregarine-like and the trophozoites described here do not resemble any life-stages of *Cryptosporidium* morphologically. To better understand, if there is any real connection between these two genera, transmission electron microscopy studies of the surface ultrastructure as well as additional sequence data from other *Polyrhabdina* species would be needed. Still, their association within this phylogeny is intriguing. This phylogenetic position confirms the uncertainty around the taxonomic placement of the genus *Polyrhabdina* within the family Lecudinidae. Originally, *Polyrhabdina* spp. were interpreted as septate eugregarines by Kamm (1922) who assigned them to a new family the Polyrhabdinidae. Reichenow (1929) combined the families Lecudinidae and Polyrhabdinidae, as he considered the septum as a misinterpretation (compare Schrével and Desportes, 2013. Later, Levine (1976) placed *P. polydorae* into the genus *Lecudina* as *L. polydorae*, but he mentioned that the species' placement is in question and needs resolving. Our results and the taxonomic history of this genus underpin the need of a comprehensive approach when identifying and describing new species (Rueckert et al., 2011). That the two *Polyrhabdina* sequences cluster away from any *Lecudina* sequence reinforces the validity of the genus. More sequences of *Polyrhabdina* and closely related gregarine species will be needed to really clarify and understand their phylogenetic position.

This is the first parasitological study on polychaetes encompassing both morphological and molecular data in the species identification, as well as the parasitological indices of infection. All polychaetes species showed high infection prevalences and mean intensities for gregarine apicomplexans (*D.* cf. *flava*: P 100%, I 80; *S. quadrisetosa*: P 100%, I 60; *B. proboscidea*: P 60%, I 38). Even though these polychaetes thrive in the same environments, our results showed a high host specificity of the gregarine species, as none of the polychaete hosts shared the same gregarine species. Similar results from different host organisms were reported in other studies (i.e. Clopton et al., 1992; Clopton and Gold, 1996; Rueckert and Leander, 2008; Clopton, 2009). Gregarines such as *S.* cf. *axiferens* and *P.* aff. *polydorae* identified in the present study from *D.* cf. *flava* have been already reported based only on morphological characteristics for *D.* cf. *flava* (syn. *Polydora flava*) from the English Channel, North-East Atlantic (Caullery and Mesnil, 1914; MacKinnon and Ray, 1931; Fowell, 1936a, 1936b). The spionid *D.* cf. *flava* is a

Table 3
Morphological comparison of *Polyrhabdina* (Apicomplexa) species presented in this study (highlighted in bold) and all other previously described species.

Polyrhabdina species	Polychaete host (accepted names)	Locality	Trophozoite shape	Trophozoite size (L × W. µm)	Nucleus shape	Nucleus size (L × W. µm)	Position of nucleus	Motility	Number of long. epicytic folds	Transverse surface folds	Shape of mucron	SSU rDNA sequence available	Literature
Polyrhabdina spionis (von Kölliker, 1848) Mingazzini, 1891	*Malacoceros fuliginosus* (Claparède, 1870)	E. Atlantic	Spindle-shaped, broad middle, pear-shaped	50–100 × 12–35	Spherical	Unknown	Middle	Contraction/ gliding	Unknown	No	8–10 prongs (more or less developed)	No	Kölliker (1848), Caullery and Mesnil (1897)
P. bifurcata Mackinnon & Ray, 1931	*Malacoceros fuliginosus* (Claparède, 1870)	E. Atlantic	Sack-like	18 × 36	Ellipsoidal	10.5 × 7.5	Middle	Immobile	Unknown	No	Knob-shaped, two large claws and 14–16 min teeth	No	Mackinnon and Ray (1931)
P. brasili Caullery & Mesnil, 1914	*Spio martinensis* Mesnil, 1896	E. Atlantic	Spindle-shaped, broad middle, pear-shaped	200 × 35	Spherical	Unknown	Middle	Contraction/ gliding	Unknown	No	8 short prongs (less developed)	No	Caullery and Mesnil (1914)
P. minuta Ganapati, 1946	*Prionospio cirrifera* Wirén, 1883	Indian Ocean	Pear-shaped	30–60 × 20	Spherical	Unknown	Middle	Unknown	Unknown	No	Short cylinder, 8 prongs/claws	No	Ganapati (1946)
P. polydorae Léger, 1893	*Polydora ciliata (Johnston, 1838) Dipolydora flava* (Claparède, 1870)	E. Atlantic	Ellipsoidal/ sack-like	100–180 × 30–40	Spherical	15	Middle	Unknown	Unknown	No	Knob-like, 22–24 prongs	No	Léger (1893), Mackinnon and Ray (1931)
P. pygospionis Caullery & Mesnil, 1914	*Pygospio elegans* Claparède, 1863	E. Atlantic	Unknown	unknown	Unknown	Unknown	Unknown	Unknown	Unknown	No	Unknown	No	Caullery and Mesnil (1914)
P. aff. *polydorae*	***Dipolydora* cf. *flava*** (Claparède, 1870)	**SW. Atlantic**	**Oval/ ellipsoidal**	**90–297 × 34–135**	**Spherical**	**14–29**	**Middle**	**Gliding**	**Up to 190**	**No**	**Flat/rounded protrusion**	**Yes**	**This study**
***P. madrynense* sp. n.**	***Spio quadrisetosa*** Blake, 1983	**SW. Atlantic**	**Rhomboid to ellipsoid**	**31–385 × 10–76**	**spherical**	**5–26**	**Close to either end of the cell**	**Gliding**	**80–150**	**No**	**Flat/knob-like protrusion, sometimes with ~ 10 prongs**	**Yes**	**This study**

common inhabitant of soft sediments of intertidal of Puerto Madryn, Argentina (M.E. Diez, unpublished data). *Dipolydora flava* was originally described from the Gulf of Naples, Mediterranean Sea, Italy. Later, it was reported from northern Europe and then from Argentina and Uruguay (Blake, 1983). This species could be an introduced species because of its disjoint distribution, but it is not been studied yet. In the case of the likely introduced *D.* cf. *flava,* molecular analyses of the gregarines species from its host native area are needed in order to confirm these species identity. The identification of *S. patagonica* sp. n. from *B. proboscidea,* which has been recently introduced to the intertidal of Puerto Madryn (M.E. Diez, unpublished data), is exciting. We would expect to find gregarine apicomplexan species of *B. proboscidea* from its native area. The only parasites reported for *B. proboscidea* from its native habitat in Southern California, United States of America, is a gregarine of the genus *Selenidium* and an unidentified mesozoan (Douglas and Jones, 1991). There is need to clarify, if we are dealing with a parasite spillover (transfer of parasites from introduced hosts to native hosts) or a spillback (transfer of native parasites to introduced hosts) effect by identifying the parasite species of *B. claparedei,* a native spionid species in Patagonia and the gregarine species of *B. proboscidea* from its native habitat. The invasion of this polychaetes species is progressive and its high densities might cause severe impacts on the community in the future (i.e. smothering barnacles and mussels on rocky substrates, burrowing into intertidal abrasion platforms, and the extinction of the native species *B. claparedei* (Kinberg, 1866)), as well as an increase in the intensity of its gregarine species. In this sense, a more neglected field of research remains to be addressed; the indirect threats invasive species can pose to the native fauna including interactions such as spillback and spillover of parasites.

5. Taxonomic summary

Phylum Apicomplexa Levine, 1970
Subphylum Sporozoa Leuckart, 1879
Class Gregarinea J.A.O. Bütschli, 1882, stat. nov. Grassé, 1953
Order Eugregarinorida Léger, 1900
Family Lecudinidae Kamm, 1922 emended Reichenow (1929)
Genus *Polyrhabdina* Mingazzini, 1891
Polyrhabdina madrynense Rueckert, Glasinovich, Diez, Cremonte & Vázquez **sp. n.**
Description. Trophozoites rhomboid or ellipsoid; mean length 142 μm (range 31–385 μm), and mean width 37 μm (range 10–76 μm); anterior and posterior end rounded, some with knob-like protrusion at the anterior end; brownish in colour. Spherical nucleus (13 μm) situated towards the ends of the trophozoites. Longitudinally oriented epicytic folds. Prongs at the base of the mucron. Trophozoites capable of gliding. Small subunit rDNA sequence is GenBank accession no. MH697739.
Type locality. Intertidal zone in Puerto Madryn (42°20′S, 64°35′W), Chubut, Argentina.
Type habitat. Marine.
Type host. *Spio quadrisetosa* Blake, 1983 (Annelida, Polychaeta, Spionidae).
Site of infection. Intestinal lumen.
Holotype. The name-bearing type of this species is the specimen shown in Fig. 3B (see Iconotype). This is in accordance with Declaration 45 recommendations to article 73 of the ICZN.
Iconotype. Fig. 3.
Etymology. Refers to the area where the polychaete host species was collected.
Order Archgregarinorida Grassé, 1953
Family Selenidiidae Brasil, 1907
Genus *Selenidium* Giard, 1884
Selenidium patagonica Rueckert, Glasinovich, Diez, Cremonte & Vázquez **sp. n.**
Description. Trophozoites vermiform; mean length 140 μm (range 112–170 μm), mean width 16 μm (range 11–20 μm); brownish in colour. Cell tapers into a rounded mucron at the anterior with slight protrusion and a tapered posterior end. Spherical nucleus (11 μm diameter) in the middle of the trophozoite. Longitudinally oriented epicytic folds. The trophozoites capable of bending and twisting. Small subunit rDNA sequence is GenBank accession no. MH697736.
Type locality. Intertidal zone in Puerto Madryn (42°20′S, 64°35′), Chubut, Argentina.
Type habitat. Marine.
Type host. *Boccardia proboscidea* Hartmann, 1940 (Annelida, Polychaeta, Spionidae).
Site of infection. Intestinal lumen.
Holotype. The name-bearing type of this species is the specimen shown in Fig. 4B (see Iconotype). This is in accordance with Declaration 45 recommendations to article 73 of the ICZN.
Iconotype. Fig. 4.
Etymology. Refers to the region where the polychaete host was collected.

Acknowledgments

Financial support was provided by the Agencia Nacional de Promoción Científica y Tecnológica Tecnológica (Préstamo BID PICT 2013- 1702, 2582 and 2016-0653) and by Consejo Nacional de Investigaciones Científicas y Técnicas (CONICET) (PIP 0670/14).

Appendix A. Supplementary material

Supplementary data to this article can be found online at https://doi.org/10.1016/j.jip.2018.10.010.

References

Blake, J.A., 1983. Polychaetes of the family Spionidae from South America, Antarctica and adjacente seas and islands. Biology of the Anarctic Seas XIV. Antarct. Res. Ser. 39, 205–288.
Brasil, L., 1909. Documents sur quelques sporozoaires d'Annélides. Arch. Protistenkunde 16, 107–142.
Bush, A.O., Lafferty, K.D., Lotz, J.M., Shostak, A.W., 1997. Parasitology meets ecology on its own terms: Margolis et al. revisited. J. Parasitol 83, 575–583.
Cardell, M.J., Sardá, R., Romero, J., 1999. Spatial changes in sublittoral soft-bottom polychaete assemblages due to river inputs and sewage discharges. Acta Oecol. 20, 343–351.
Caullery, M., Mesnil, F., 1897. Sur un type nouveau (*Metchnikovella* n.g.) d'organismes parasites de grégarines. C. R. l'Acad Sci. Paris 125, 785–790.
Caullery, M., Mesnil, F., 1899. Sur quelques parasites internes des Annélids. I. Les grégarines nématoides des Annélids: G. *Selenidium* Giard. Traveaux de la Station Zoologique de Wimereux 7, 80–99.
Caullery, M., Mesnil, F., 1914. Sur l'existence de gregarines dicystidées chez les annelids polychàetes. C. R. Soc. Biol. Paris 77, 516–520.
Clopton, R.E., 2009. Phylogenetic relationships, evolution, and systematic revision of the septate gregarines (Apicomplexa: Eugregarinorida: Septatorina). Comp. Parasitol. 76, 167–190.
Clopton, R.E., Gold, R.E., 1996. Host specificity of *Gregrina blattarum* von Siebold, 1839 (Apicomplexa: Eugregarinida) among five species of domiciliary cockroaches. J. Invertebr. Pathol. 67, 219–223.
Clopton, R.E., Percival, T.J., Janovy, J.R., 1992. Host stadium specificity in the gregarine assemblage parasitizing *Tenebrio molitor*. J. Parasitol. 78, 334–337.
Desportes, I., Schrével, J., 2013. Gregarines, The early branching Apicomplexa. 2013. In: Treatise on Zoology, Anatomy, Taxonomy, Biology. BRILL, Leiden – The Netherlands, vol. 1, pp. 197–375.
Douglas, T.G., Jones, I., 1991. Parasites of California spionid polychaetes. Bull. Mar. Sci. 48, 308–317.
Fauchald, K., 1977. The polychaete worms, definitions and keys to the orders, families and genera. Nat. Hist. Mus. Los Angeles Cry Sci. Ser. 28, 1–188.
Fowell, R.R., 1936a. The fibrilar structures of Protozoa with special reference to schizogregarines of the genus *Selenidium*. J. R. Microsc. Soc. 58, 12–28.
Fowell, R.R., 1936b. Observations on the sporozoa inhabiting the gut of the polychaete worm *Polydora flava* Claparède. Parasitology 28, 414–430.
Ganapati, P.N., 1946. Notes on some gregarines from polychaetes of the Madras coast. Proc. Indian Acad. Sci. 23, 228–248.
Giard, A., 1884. Sur un nouveau groupe de protozoaires parasites d'annélides polychètes et sur quelques points de l'histoire des grégarines (*Selenidium pendula*). C.R. Ass. Fr. Avanc. Sci. Congrès de Blois 192.
Grassé, P.P., 1953. Classe des grégarinomorphes (Gregarinomorpha, N. nov., Gregarinae

Haeckel, 1866; gregarinidea Lankester, 1885; grégarines des auteurs). In: Grassé, P.P. (Ed.), Traité de Zoologie. Masson, Paris, pp. 590–690.
Guindon, S., Gascuel, O., 2003. A simple, fast, and accurate algorithm to estimate large phylogenies by maximum likelihood. Syst. Biol. 52, 696–704.
Guindon, S., Dufayard, J.F., Lefort, V., Anisimova, M., Hordijk, W., Gascuel, O., 2010. New algorithms and methods to estimate maximum-likelihood phylogenies: Assessing the performance of PhyML 3.0. Syst. Biol. 59, 307–321.
Huelsenbeck, J.P., Ronquist, F., 2001. MrBayes: Bayesian inference of phylogenetic trees. Bioinformatics 17, 754–755.
Iritani, D., Wakeman, K.C., Leander, B.S., 2018. Molecular phylogenetic positions of two new marine gregarines (Apicomplexa) –*Paralecudina anankea* n. sp. and *Lecudina caspera* n. sp. – from the intestine of *Lumbrineris inflata* (Polychaeta) show patterns of co-evolution. J. Eukaryot. Microbiol. 65, 211–219.
Jaubet, M.L., Garaffo, G.V., Vallarino, E.A., Elías, R., 2015. Invasive polychaete *Boccardia proboscidea* Hartman, 1940 (Polychaeta: Spionidae) in sewage-impacted areas of the SW Atlantic coasts: morphological and reproductive patterns. Mar. Ecol. 36, 611–622.
Kamm, M.E., 1922. Studies on gregarines II. Synopsis of the polycystid gregarines of the world excluding those from Myriapoda, Orthoptera, and Coleoptera. Illinois Biol. Monogr. 7, 1–104.
Kölliker, A., 1848. Beiträge zur Kenntnis der niederen Thiere.Ueber die Gattung Gregarina L Duf. Zeitsch. f. wissensch. Zoologie 1, 1–47.
Kuvardina, O., Simdyanov, T., 2002. Fine structure of syzygy in *Selendium pennatum*. Protistology 2, 169–177.
Leander, B.S., 2006. Ultrastructure of the archigregarine *Selenidium vivax* (Apicomplexa): a dynamic parasite of sipunculid worms (Host: *Phascolosoma agassizii*). Mar. Biol. Res. 2, 178–190.
Leander, B.S., 2007. Molecular phylogeny and ultrastructure of *Selenidium serpulae* (Apicomplexa, Archigregarinia) from the calcareous tubeworm *Serpula vermicularis* (Annelida, Polychaeta, Sabellida). Zool. Scr. 36, 213–227.
Leander, B.S., 2008. Marine gregarines—evolutionary prelude to the apicomplexan radiation? Trends Parasitol. 24, 60–67.
Leander, B.S., Lloyd, S.A.J., Marshall, W., Landers, S.C., 2006. Phylogeny of marine gregarines (Apicomplexa) - *Pterospora*, *Lithocystis* and *Lankesteria* -and the origin (s) of coelomic parasitism. Protist 157, 45–60.
Léger, L., 1893. Lévolution des gregarines intestinales des vers marine. C. R. Acad. Sci. 116, 204–206.
Levine, N.D., 1971. Taxonomy of the Archigregarinorida and Selenidiidae (Protozoa, Apicomplexa). J. Protozool. 18, 704–717.
Levine, N.D., 1976. Revision and checklist of the species of the aseptate gregarine genus *Lecudina*. Trans. Am. Microsc. Soc. 95, 695–702.
Levine, N.D., 1979. New genera and higher taxa of septate gregarines (Protozoa, Apicomplexa). J. Protozool. 26, 532–536.
Lord, J.C., Omoto, C.K., 2012. Eugregarines reduce susceptibility of the hide beetle, *Dermestes maculatus*, to apicomplexan pathogens and retard larval development. J. Invertebr. Pathol. 111, 186–188.
Mackinnon, D.L., Ray, H.N., 1931. Observations on dicystid gregarines from marine worms. Quart. J. Microsc. Sci. 74, 439–466.
Maddison, D.R., Maddison, W.P., 2005. MacClade 4.08. Sinauer Associates, Sunderland.
Miller, M.A., Pfeiffer, W., Schwartz, T., 2010. Creating the CIPRES Science Gateway for inference of large phylogenetic trees. In: Proceedings of the Gateway Computing Environments Workshop (GCE), New Orleans, LA, pp. 1–8.
Nybakken, J.W., Bertness, M.D., 2005. Estuaries and salt marshes. In: Nybakken, J.W., Bertness, M.D. (Eds.), Marine Biology: An Ecological Approach. Pearson/Benjamin Cummings, San Francisco, pp. 1–579.
Posada, D., Crandall, K.A., 1998. MODELTEST: testing the model of DNA substitution. Bioinformatics 14, 817–818.
Ray, H.N., 1930. Studies on some protozoa in polychaete worms. I. Gregarines of the genus *Selenidium*. Parasitology 22, 370–400.
Reichenow, E., 1929. Sporozoa, Lehrbuch der Protozoenkunde. Jena 863–1153.
Romero, M.A., Sánchez, F., Sabino, M.A., Rodríguez, J.P., González, G., Noris-Suarez, K., 2011. Biocompatibility study on substrates fabricated for nerve guides using scanning electron microscopy and comparing two drying sample methods. Acta Microsc. 20, 131–140.
Rouse, G.W., Pleijel, F., 2001. Polychaetes. Oxford University Press, Oxford, pp. 354.
Rueckert, S., Horàk, A., 2017. Archigregarines of the English Channel revisited: New molecular data on *Selenidium* species including early described and new species and the uncertainties of phylogenetic relationships. PLoS One 12, e0187430.
Rueckert, S., Leander, B.S., 2008. Morphology and phylogenetic position of two novel marine gregarines (Apicomplexa, Eugregarinorida) from the intestines of North-eastern Pacific ascidians. Zool. Scr. 37, 637–645.
Rueckert, S., Leander, B.S., 2009. Molecular phylogeny and surface morphology of marine archigregarines (Apicomplexa) - *Selenidium* spp., *Filipodium phascolosomae* n. sp. and *Platyproteum* n. gen. et comb.- from North-eastern Pacific peanut worms (Sipuncula). J. Eukaryot. Microbiol. 56, 428–439.
Rueckert, S., Leander, B.S., 2010. Description of *Trichotokara nothriae* n. gen. et sp. (Apicomplexa, Lecudinidae) – An intestinal gregarine of *Nothria conchylega* (Polychaeta, Onuphidae). J. Invert. Path. 104, 172–179.
Rueckert, S., Chantangsi, C., Leander, B.S., 2010. Molecular systematics of marine gregarines (Apicomplexa) from North-eastern Pacific polychaetes and nemerteans, with descriptions of three novel species: *Lecudina phyllochaetopteri* sp. nov., *Difficilina tubulani* sp. nov. and *Difficilina paranemertis* sp. nov. Int. J. Syst. Evol. Microbiol. 60, 2681–2690.
Rueckert, S., Villette, P.M.A.H., Leander, B.S., 2011. Species boundaries in gregarine apicomplexans: a case study comparison of morphometric and molecular variability in *Lecudina* cf. *tuzetae* (Eugregarina, Lecudinidae). J. Eukaryot. Microbiol. 58, 275–283.
Schrével, J., 1970. Contribution à l'étude des Selenidiidae parasites d'annélides polychaètes. I. Cycles biologiques. Protistologica 6, 389–426.
Schrével, J., 1971. Observations biologiques et ultrastructurales sur les Selenidiidae et leurs conséquences sur la systématique des Grégarinomorphes. J. Protozool. 18, 448–470.
Schrével, J., Desportes, I., 2013. Marine gregarines. In: Desportes, I., Schrével, J. (Eds.) Gregarines, The early branching Apicomplexa. 2013. Treatise on Zoology, Anatomy, Taxonomy, Biology. BRILL, Leiden – The Netherlands, vol. 1, pp. 197–375.
Schrével, J., Valigurová, A., Prensier, G., Chambouvet, A., Florent, I., Guillou, L., 2016. Ultrastructure of *Selenidium pendula*, the type species of archigregarines, and phylogenetic relations to other marine Apicomplexa. Protist 167, 339–368.
Simdyanov, T.G., 2009. *Difficilina cerebratuli* gen. et sp. n. (Eugregarinida: Lecudinidae) - a new gregarine species from the nemertean *Cerebratulus barentsi* Bürger, 1895 (Nemertini: Cerebratulidae). Parazitologiya 43, 273–287.
Sun, X., Peng, Q., Wu, W., Zhang, G., 2012. Characterization of a coelomic gregarine parasite from *Thitarodes pui* (Lepidoptera: Hepialidae) in the Tibetan Plateau. J. Invertebr. Pathol. 11, 160–165.
Vivier, E., Schrével, J., 1966. Les ultrastructures cytoplasmiques de *Selenidium hollandei*, n.sp., gregarine parasite de *Sabellaria alveolata* L. J. Microsc. (Paris) 5, 213–228.
Vivier, E., Desportes, I., 1990. Phylum Apicomplexa. In: Margulis, L., Corliss, J.O., Melkonian, M., Chapman, D.J. (Eds.), Handbook of Protoctista. Jones and Bartlett Publ, Boston, Massachusetts, pp. 549–573.
Wakeman, K.C., Leander, B.S., 2012. Molecular phylogeny of Pacific archigregarines (Apicomplexa), including descriptions of *Veloxidium leptosynaptae* n. gen., n. sp., from the sea cucumber *Leptosynapta clarki* (Echinodermata), and two new species of *Selenidium*. J. Eukaryot. Microbiol. 59, 232–245.
Wakeman, K.C., Leander, B.S., 2013. Molecular phylogeny of marine gregarine parasites (Apicomplexa) from tube-forming polychaetes (Sabellariidae, Cirratulidae, and Serpulidae), including descriptions of two new species of *Selenidium*. J. Eukaryot. Microbiol. 60, 514–525.
Zwickl, D., 2006. Genetic Algorithm Approaches for the Phylogenetic Analysis of Large Biological Sequence Datasets Under the Maximum Likelihood Criterion. PhD thesis. University of Texas at Austin, pp. 125.